INVITED PAPER *Special Section on Multidisciplinary and Innovative Key technologies in Advanced communication systems (MIKA)*

Communication Quality Estimation Observer: An Approach for Integrated Communication Quality Estimation and Control for Digital-Twin-Assisted Cyber-Physical Systems

Ryogo KUBO[†a)], ***Member***

SUMMARY Cyber-physical systems (CPSs) assisted by digital twins (DTs) integrate sensing-actuation loops over communication networks in various infrastructure services and applications. This study overviews the concept, methodology, and applications of the integrated communication quality estimation and control for the DT-assisted CPSs from both communications and control perspectives. The DT-assisted CPSs can be considered as networked control systems (NCSs) with virtual dynamic models of physical entities. A communication quality estimation observer (CQEO), which is an extended version of the communication disturbance observer (CDOB) utilized for time-delay compensation in NCSs, is proposed to estimate the integrated effects of the quality of services (QoS) and cyberattacks on the NCS applications. A path diversity technique with the CQEO is also proposed to achieve reliable NCSs. The proposed technique is applied to two kinds of NCSs: remote motor control and haptic communication systems. Moreover, results of the simulation on a haptic communication system show the effectiveness of the proposed approach. In the end, future research directions of the CQEO-based scheme are presented.

key words: *communication quality, networked control system, disturbance observer, digital twin, cyber-physical system*

1. Introduction

A cyber-physical system (CPS) only functions if information, communications, and control technologies are integrated [1], [2]. In particular, sensing and actuation over communication networks are key techniques for building more sophisticated and diversified CPSs. From a control perspective, the CPS can be considered as a networked control system (NCS) [3]–[5], in which controllers, sensors, and actuators are connected through communication networks. Therefore, the system performance and stability are significantly affected by network-induced constraints such as time delays, packet losses, sampling intervals, data quantization, and network security [6], [7]. These network-induced imperfections in the NCSs have stimulated multidisciplinary studies on information, communications, and control engineering in recent years [8]–[12].

To reduce the time delays for delay-sensitive CPS applications, such as teleoperation, augmented reality, serious gaming, and smart grid, the concept of the tactile internet (TI) has been proposed from a communications perspective [13]. TI is aimed at achieving a 1-ms end-to-end latency, for example, by using multi-access edge computing (MEC) [14]. As for wired networks, various edge computing architectures based on passive optical networks (PONs) have been proposed [15]–[17] for medical and robotic applications. Maier et al. [18] proposed a TI architecture using fiber wireless (FiWi)–enhanced mobile networks for a teleoperation system. The TI is expected to become an ultra reliable and low latency communications (URLLC) service in the beyond-5G or 6G era [19].

The TI will enable the ultra-low-latency CPS services by using the MEC-based architecture. However, the MEC-based architecture assumes the locality of distributed physical entities. In fact, it is difficult to achieve cooperative control of devices distributed over a wide area and teleoperation from distant locations. Therefore, in addition to adopting a TI-based approach, application and network control techniques to overcome the network constraints such as time delays in CPSs are necessary. The network-level communication quality can be estimated as the quality of services (QoS), for example, latency, packet loss rate, and throughput. Park et al. [20] proposed a robust multipath selection algorithm based on the round-trip time (RTT) for a CPS. Furthermore, various QoS-based network control and data transmission schemes for NCSs have been discussed [21]–[23]. At the application level, the QoS information has been also utilized to compensate for the effects of time delays in NCSs [24]–[26].

Although the QoS-based control schemes can theoretically achieve robust and reliable NCSs, the measurement and estimation of each QoS metric are often difficult. Therefore, it is worth estimating and controlling the integrated communication quality at the application level in NCSs. A digital twin (DT) has recently emerged as a promising tool to estimate the integrated communication quality. The DT is a virtual model of a physical system and can be used to predict, optimize, and control future behavior of entities in the system [27]–[29]. Newrzella et al. [30] classified the DT concept across industries, in which there have been various definitions of the DT. The DT-assisted CPSs have been proposed for various applications, including the manufacturing system [31], on-orbit spacecraft [32], and smart grids [33]. The DT concept covers not only model-based approach but also data-driven approach in that modeling errors can be observed by real-time communication between a virtual model

Manuscript received November 26, 2021.
Manuscript revised February 4, 2022.
Manuscript publicized April 14, 2022.

[†]The author is with the Department of Electronics and Electrical Engineering, Keio University, Yokohama-shi, 223-8522 Japan.
a) E-mail: kubo@elec.keio.ac.jp

DOI: 10.1587/transcom.2021MEI0003

and a physical entity. Moreover, not only an analytical model of a physical entity but also a simulator can be utilized as a DT in complicated systems that are difficult to model, such as multi-agent systems. In that sense, this paper uses the term of DT-assisted CPS while a simplified analytical model is utilized for illustration purpose in this study. In the DT-assisted CPSs, the effects of the network-induced constraints can be mitigated by application and network control based on the integrated communication quality at the application level if the system modeling is possible, for example, by using sophisticated machine learning techniques.

Natori et al. [34], [35] proposed a communication disturbance observer (CDOB) to compensate for the effects of time delays on NCSs. The CDOB does not need any time-delay models in the system and is effective for not only constant but also time-varying delays. The CDOB estimates the effects of time delays as a disturbance at the application level by using a nominal model of a controlled subsystem, which can be considered as a simplified DT. A double disturbance observer (DDOB) was proposed to cope with the modeling errors in the CDOB-based time-delay compensation [36], [37]. The CDOB-based NCSs are affected by not only time delays but also packet losses [38]. The effects of packet losses on NCSs can be also considered as a disturbance [39]. The CDOB can estimate the integrated communication quality, including both time delays and packet losses as a disturbance [40], [41]. As for the NCSs with the CDOB, the steady-state errors caused by time-varying delays and packet losses have been discussed [42], [43]. In addition, a modified CDOB was proposed to compensate for the effects of data losses caused by sleep-based energy-efficient network interfaces [44]. Moreover, Lee et al. [45] proposed a fuzzy-based CDOB architecture based on neural network modeling. In this architecture, a learning algorithm is utilized to perform system identification.

The above-mentioned CDOBs involve techniques for application control in NCSs. The CDOB is also effective for network control, for example, for path selection in multipath routing. The disturbance estimated by the CDOB includes the effects of time delays, jitter, packet loss, etc. This means that the disturbance indicates the integrated communication quality at the application level [46]. However, the integrated communication quality estimation based on the CDOB has not been applied to network control. Recently, cybersecurity in NCSs has been recognized as a critical issue [47]. Various attack scenarios, such as false data injection (FDI) attacks, replay attacks, and denial-of-service (DoS) attacks, have been studied [48]. The effects of FDI-based cyberattacks against the NCSs can be also considered as disturbance. To detect and mitigate data tampering attacks in the NCSs, a tamper detection observer (TDO) was proposed [49], [50]. The TDO includes an algorithm to select a path that has not been attacked out of multiple paths based on observer-based disturbance estimation. The communication quality estimation through the CDOB as well as TDO should be applied to network control, and in this study, we discuss the integrated communication quality, including the effects of both QoS and cybersecurity.

The observer-based approach to estimating the integrated communication quality has been applied to various NCSs. For example, a haptic communication system is one of the interactive NCSs [51]. Master and slave haptic devices are bilaterally controlled over networks. To compensate for the effects of time delays, the configuration of the CDOB for the bilateral control was discussed in [52]. In addition, the configuration of the TDO was discussed in [53] and [54] to detect and mitigate data tampering attacks. Moreover, network control techniques based on the QoS for haptic communication systems have been studied. Furthermore, multipath routing techniques were proposed to improve the reliability of the system in [55] and [56]. A server selection technique based on the QoS information was also proposed in [57]. In haptic communication systems, however, the integrated communication quality estimation based on the CDOB has not been applied to network control.

This study overviews the concept, methodology, and applications of the integrated communication quality estimation and control for the DT-assisted CPSs from both communications and control perspectives. A communication quality estimation observer (CQEO), which is an extended version of the CDOB, is proposed to estimate the integrated effects of the QoS and cyberattacks on various NCS applications. The CQEO is configured with multiple network paths and a nominal model of a controlled subsystem. We also propose a CQEO-based network control technique using path diversity to achieve reliable NCSs. Figure 1 summarizes the proposed approach, more traditional approaches, and the CDOB-based approach. The proposed CQEO is applied to two types of NCSs: remote motor control and haptic communication systems. We perform simulations on the haptic communication system; the results confirm the effectiveness of the proposed technique.

This rest of the paper is organized as follows: The immediately following section describes the concept of the DT-assisted CPSs and its modeling. Section 3 describes the communication quality estimation and control schemes using the CDOB and CQEO. Section 4 describes the imple-

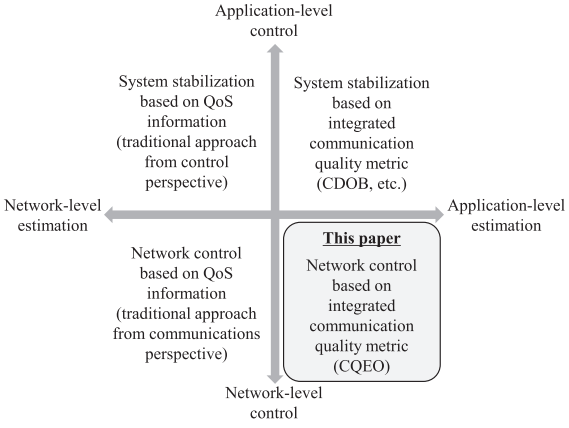

Fig. 1 Classification of communication quality estimation and control.

mentation of the CQEO into the path diversity technique for client-server NCSs, taking a remote motor control system as an example. Section 5 describes the implementation of the CQEO into the path diversity technique for peer-to-peer NCSs, taking a haptic communication system as an example. The results of the simulation on the haptic communication system are shown in Sect. 6. Finally, in Sect. 7, we present our conclusions and directions for future research.

2. DT-Assisted CPS and Its Modeling

This section describes the concept of the DT-assisted CPS, its modeling as a CPS service, and a disturbance observer (DOB) for disturbance rejection.

2.1 Concept of DT-Assisted CPS

The concept of the DT-assisted CPSs are illustrated in Fig. 2. The DT-assisted CPSs can be broadly classified into client-server and peer-to-peer CPSs. In the client-server CPS, as shown in Fig. 2(a), the controllers are located on the network-side cyber space, and the physical subsystems including sensors and actuators are controlled over the networks. The DTs of the controlled subsystems are generated in the centralized or distributed servers. In addition, the local DTs are generated in the distributed devices including sensors and actuators. In the peer-to-peer CPS, as shown in Fig. 2(b), the controllers are located on the local cyber space, and the distributed devices including sensors and actuators are controlled multilaterally over the networks. Moreover, the DTs of peer subsystems are generated in the distributed devices.

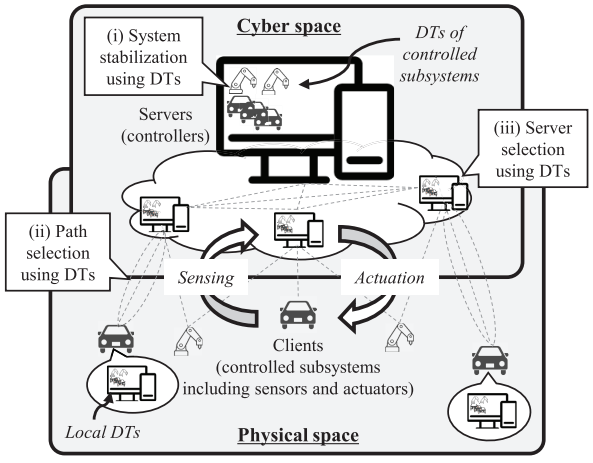

(a) Client-Server CPS

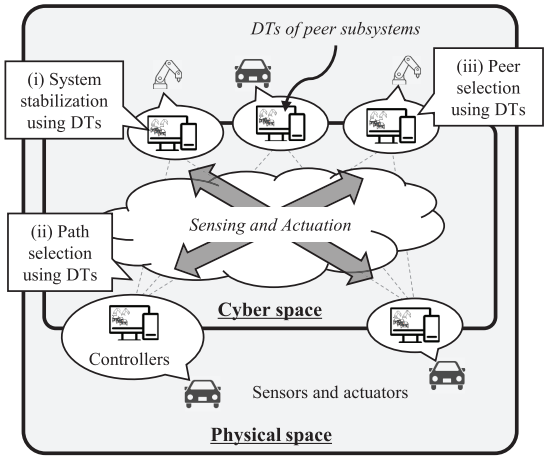

(b) Peer-to-Peer CPS

Fig. 2 Concept of the DT-assisted CPSs.

The DT-assisted CPSs enable the following three functions to control the communication quality without direct QoS measurement at the network level. First, model-based predictive QoS compensation techniques can be implemented at the application level to stabilize the system. For example, the CDOB estimates and compensates for the effects of time delays by using the DT-based prediction. Second, multipath routing techniques can be implemented at the network level to achieve an appropriate path selection. For example, the CQEO-based network control technique using path diversity estimates the integrated communication quality in each path by using the DT-based prediction, and selects the path with the best communication quality. Third, controller allocation techniques can be implemented at the network level to achieve an appropriate server selection. For example, the CQEO-based network control technique estimates the integrated communication quality for each server by using the DT-based prediction, and selects the server with the best communication quality.

This study mainly focuses on the CQEO-based network control technique using path diversity for the client-server and peer-to-peer NCSs. A remote motor control system and a haptic communication system are taken as examples of the client-server and peer-to-peer NCSs, respectively.

2.2 DT-Assisted Networked Control as a CPS Service

If the DT-assisted feedback control over communication networks is considered as one of the CPS services, the system can be illustrated as Fig. 3. The feedback controller and physical plants, that is, the controlled subsystem including a sensor and an actuator, are connected over the forward and feedback networks. A proportional-integral-derivative (PID)–based controller can be implemented as the feedback

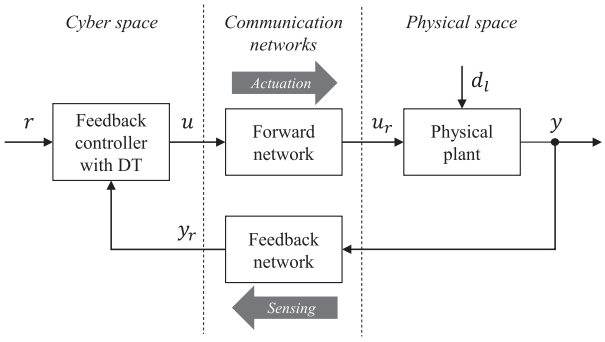

Fig. 3 Configuration of the DT-assisted NCS.

controller. The controller is designed based on the DT, that is, a model of the physical plant, which can be updated static or dynamically. In Fig. 3, r, u, and y denote the reference, control input, and response, respectively. The subscript r denotes the signal received over a network, where the packetized signal can be delayed or lost.

In general, the local disturbance d_l including modeling errors is input to the control system. In a motor control system, for example, the disturbance includes the inertia fluctuation, frictional torque, and load torque, which cannot be completely modelled in advance. As local disturbance affects not only the system stability and performance but also communication quality estimation as will be discussed hereafter, it becomes important to completely reject the local disturbance so that the physical plant works the same way as the DT.

2.3 DT-Assisted Disturbance Rejection Using DOB

The DT of the physical plant has modeling errors even if the DT is updated based on real-time machine learning. The DOB estimates the system uncertainties or modeling errors, as disturbance d_l. The DOB has been utilized to improve the robustness against the disturbance in various practical control systems [58], [59]. The nominal model of the physical plant in the DOB can be considered as a DT. The merit of using the DOB lies in the simple implementation compared with other robust control schemes.

The overview of the DT-assisted disturbance rejection using the DOB is shown in Fig. 4. As shown in Fig. 4(a), the DOB comprises the DT and Q-filter on the plant side. The DT on the plant side, that is, local DT, is the inverse nominal model of the physical plant, which means the physical plant model without the disturbance. The Q-filter is a low-pass filter (LPF) to stabilize the system. The DOB calculates the estimated local disturbance $\hat{d}_l$ through the Q-filter and compensates for the disturbance. The compensated signal u_a is input to the physical plant. The block diagram of Fig. 4(a) can be equivalently transformed into Fig. 4(b). Therefore, disturbance d_l is input to the system through the $(1-Q)$-filter, that is, high-pass filter (HPF), by the compensation using the DOB. The Q-filter with a higher cut-off frequency achieves more robust control against the disturbance. In practice, however, increasing the cut-off frequency is limited by system noises.

For example, we consider the transfer function of a linear time-invariant (LTI) system, $G_n(s)$, where s denotes the Laplace variable, as a nominal plant. The estimated local disturbance $\hat{d}_l$ can be calculated as (1)

$$\begin{aligned}\hat{d}_l &= Q(s)\left(u_a - G_n(s)^{-1}y\right)\\ &= \frac{g_{dob}}{s+g_{dob}}d_l,\end{aligned} \tag{1}$$

where $Q(s)$ and g_{dob} denote the first-order Q-filter and its cut-off frequency, respectively. The output of the system is represented as (2)

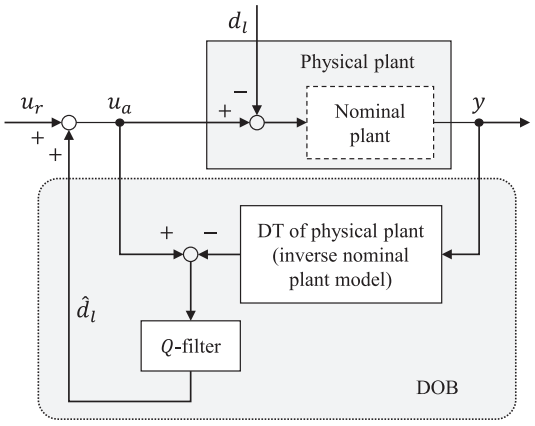

(a) Configuration of the DOB

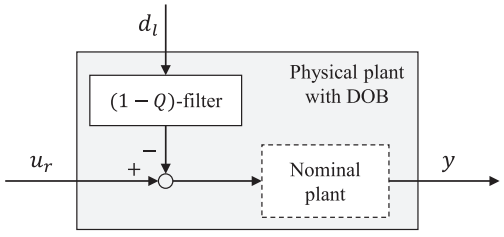

(b) Equivalent block diagram of Fig. 4(a)

Fig. 4 DT-assisted disturbance rejection using the DOB.

$$\begin{aligned}y &= G_n(s)u_r - (1-Q(s))\,d_l\\ &= G_n(s)u_r - \frac{s}{s+g_{dob}}d_l.\end{aligned} \tag{2}$$

If the cut-off frequency g_{dob} is sufficiently large, the local disturbance d_l is completely rejected. Therefore, the physical plant works the same way as the local DT or nominal plant by using the DOB. Introducing the DOB into the local subsystem enables the integrated communication quality estimation and control as will be described in the following sections.

3. Communication Quality Estimation and Control

This section describes the CDOB-based application control technique and proposed CQEO-based network control technique for the DT-assisted CPSs. These techniques are discussed based on the DT-assisted NCS shown in Fig. 3.

3.1 CDOB-Based Estimation and Application Control

The CDOB is a passive method to measure the effects of time delays at the application level and does not utilize additional traffic over the networks to measure the communication quality. The time-delay compensation technique using the CDOB at the application level is described in this section.

3.1.1 CDOB

As shown in Fig. 5(a), the physical plant with the DOB is

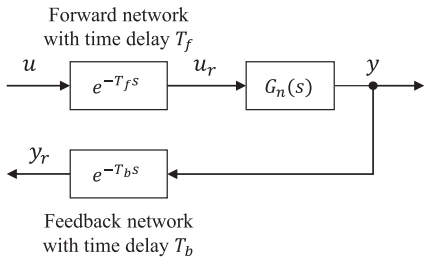

(a) Forward and feedback networks with time delays

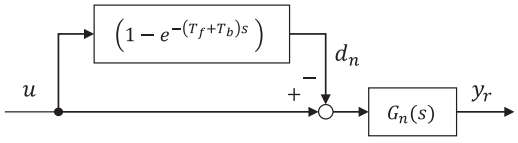

(b) Equivalent block diagram of Fig. 5(a)

Fig. 5 Time-delayed networks as a disturbance.

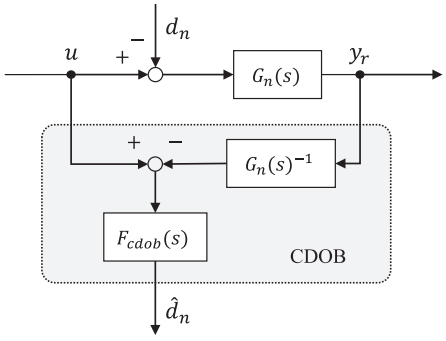

Fig. 6 Network disturbance estimation by the CDOB.

represented as the transfer function $G_n(s)$. In addition, the forward and feedback network delays are defined as T_f and T_b, respectively. The effects of the time delays can be considered as a network disturbance d_n, as shown in Fig. 5(b) and (3)

$$d_n = \left(1 - e^{-(T_f+T_b)s}\right) u. \tag{3}$$

The configuration of the CDOB is shown in Fig. 6. Similar to the DOB, the CDOB estimates the network disturbance without using any time-delay model or measurement [34], [35]. The CDOB comprises the inverse DT model of $G_n(s)$ and the LPF $F_{cdob}(s)$ on the controller side. If the DOB compensates for the local disturbance perfectly, the DT model $G_n(s)$ on the controller side, that is, remote DT, is identical to the characteristics of the physical plant. The estimated network disturbance $\hat{d}_n$ can be calculated as (4)

$$\begin{aligned}\hat{d}_n &= F_{cdob}(s)\left(u - G_n(s)^{-1} y_r\right) \\ &= \frac{g_{cdob}}{s + g_{cdob}} d_n,\end{aligned} \tag{4}$$

where $F_{cdob}(s)$ and g_{cdob} denote the first-order LPF and its cut-off frequency, respectively. The estimated network disturbance $\hat{d}_n$ indicates the effects of the time delays at the application level.

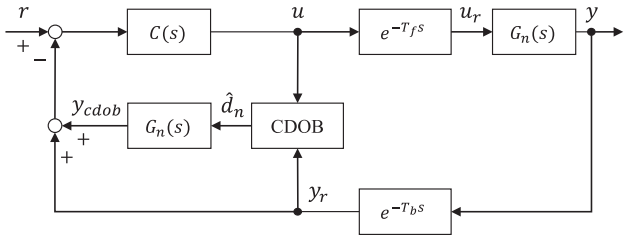

Fig. 7 Time-delay compensation by the CDOB.

3.1.2 Application-Level Control Using CDOB

In NCSs, the time-delay compensation at the application level means eliminating the time-delay elements, $e^{-T_f s}$ and $e^{-T_b s}$, from the feedback loop. The input-output transfer function of the NCS shown in Fig. 3 is calculated as (5)

$$\frac{y}{r} = \frac{C(s)G_n(s)e^{-T_f s}}{1 + C(s)G_n(s)e^{-(T_f+T_b)s}}, \tag{5}$$

where $C(s)$ denotes the transfer function of the feedback controller. The denominator of the transfer function includes the time delays, T_f and T_b, and the behavior of the system depends on the time-delay elements.

The block diagram of the NCS with the CDOB is shown in Fig. 7. The compensation value y_{cdob} is calculated as (6)

$$y_{cdob} = \frac{g_{cdob}}{s + g_{cdob}} G_n(s) d_n. \tag{6}$$

If the cut-off frequency g_{cdob} is sufficiently large, the input-output transfer function of the NCS is calculated as (7)

$$\frac{y}{r} = \frac{C(s)G_n(s)e^{-T_f s}}{1 + C(s)G_n(s)}, \tag{7}$$

because the network disturbance is cancelled by the output of the CDOB. The denominator of the transfer function does not include the time delays, T_f and T_b, and the feedback controller can be designed without considering the network elements.

3.2 CQEO-Based Estimation and Network Control

The CQEO is an active method to measure the integrated effects of communication quality at the application level by transmitting duplicated data. The path and server selection technique using the CQEOs and redundancy-based network control is described in this section.

3.2.1 CQEO

The original CDOB compensates for the effects of constant time delays in an LTI system, even without being aware of them. However, the CPSs or NCSs are affected by the integrated communication quality, including not only due to constant time delays but also jitters, packet losses, and

cyberattacks. The implementation of the CQEO aims at estimating the integrated communication quality as a disturbance at the application level. In contrast to the CDOB, the CQEO is utilized not for the QoS compensation, such as time-delay compensation, at the application level to guarantee the system stability, but for selecting the network path and control server with the best communication quality to achieve a high-availability system.

The CQEO, which uses local and remote DTs, is an extended version of the CDOB and is inspired by the state-of-the-art studies related to the CDOB, for example, studies on defining network disturbance due to jitters and packet losses [40], nominal model allocation for the CDOB to suppress the effects of jitters and packet losses [42], and observer-based cyberattack detection using redundant paths [49]. In this study, an integrated communication quality disturbance d_c is defined at the application level to model the effects of communication quality such as time delays, packet losses, and cyberattacks.

The concept of the estimation of disturbance d_c using the CQEO is illustrated in Fig. 8. The CQEO is configured over the forward and feedback networks. The communication quality disturbances of the forward and feedback networks are defined as d_{cf} and d_{cb}, respectively. The CQEO includes the two DTs of the physical plant on the controller and plant sides. The output of the DT on the controller side, that is, remote DT, is defined as y_{mc}. The output of the DT on the plant side, that is, local DT, is defined as y_m, transmitted to the controller side, and received on the controller side as y_{mr} after passing through the feedback network. The estimated communication quality disturbance $\hat{d}_c$ can be calculated as (8)

$$\hat{d}_c = y_{mc} - y_{mr}. \tag{8}$$

Disturbance d_c indicates the effects of communication quality in the forward and feedback networks on the NCS. The specific configurations of the CQEO for the client-server and peer-to-peer NCSs are discussed in Sects. 4 and 5, respectively.

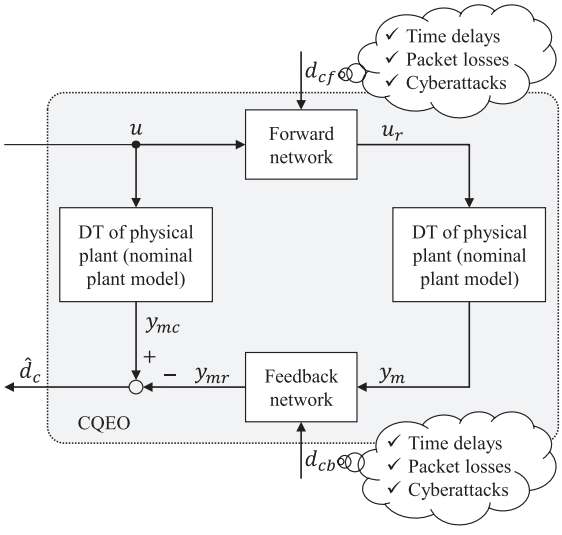

Fig. 8 Conceptual diagram of the CQEO for the DT-assisted NCS.

3.2.2 Network-Level Control Using CQEO

It can be assumed that a system has multiple forward and feedback network paths. In addition, one of the multiple distributed servers can become a controller server, where the feedback controller is implemented. The communication quality disturbance estimated by each CQEO for the combination of forward path i, feedback path j, and controller server k, $\hat{d}_{c,i,j,k}$ is utilized to achieve an appropriate path and server selection. If the numbers of forward paths, feedback paths, and controller servers are defined as n_{nf}, n_{nb}, and n_c, the system configuration for the path and server selection technique can be illustrated as Fig. 9.

As shown in Fig. 9, the operation server determines which controller server should be utilized to control the physical plant with the best performance, based on $\hat{d}_{c,i,j,k}$ for all i, j, and k. The communication protocol between the operation server and controller servers is required when there are multiple controller servers available for the NCS service. The migration mechanism for controller servers is also required to maintain continuity of control. Moreover, the path selector in controller server k determines which forward and feedback network paths should be utilized in combination to control the physical plant with the best performance, based on $\hat{d}_{c,i,j,k}$ for all i and j.

For example, the selected combination of forward and feedback paths can be determined as (9)

$$\arg\min_{i,j,k} \left| \frac{g_{cqeo}}{s + g_{cqeo}} \hat{d}_{c,i,j,k} \right|, \tag{9}$$

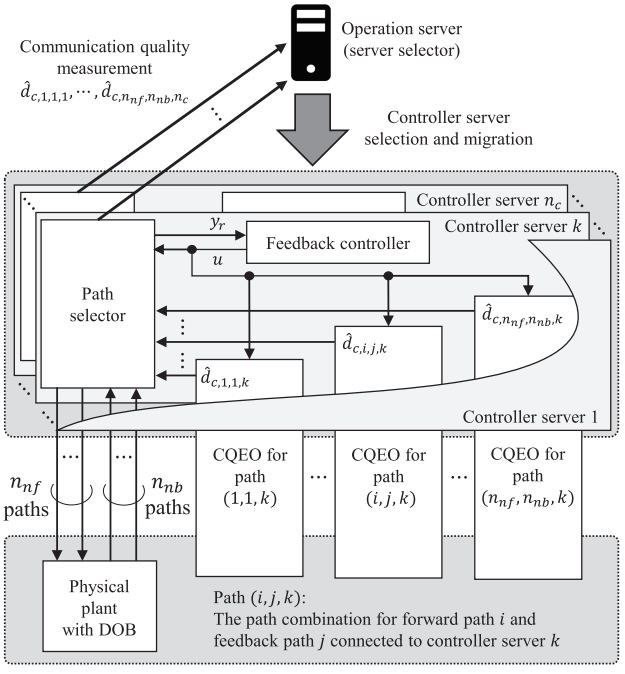

Fig. 9 Path and server selection technique with the CQEOs.

where the combination (i, j, k) indicates the path number for i-th forward path and j-th feedback path connected to k-th controller server, and g_{cqeo} denotes the cut-off frequency of the LPF to avoid frequent path switching. As this path selection algorithm is straightforward and not optimized, further studies are required to develop a more sophisticated algorithm. The forward and feedback paths determined by the path selector are utilized to transmit the control input u and response y. The specific algorithms of the path selector for the client-server and peer-to-peer NCSs are described in Sects. 4 and 5, respectively.

4. Path Diversity with CQEO for Client-Server NCSs

This section describes the CQEO-based network control technique using path diversity for the client-server NCSs by taking a remote motor control system as an example.

4.1 Networked Motion Control

A configuration of the remote position servo system is shown in Fig. 10. It is assumed that this system comprises the position controller, communication networks, current-controlled linear motor, and DOB. The position controller is implemented on the server side, and the motor and DOB are implemented on the client side. In Fig. 10, x^{cmd}, x^{res}, and I^{ref} denote the position command, position response, and current reference, respectively. The communication quality disturbances of the forward and feedback networks, $d^I_{c,f}$ and $d^x_{c,b}$, include the effects of time delays, packet losses, and cyberattacks. The received values for I^{ref} and x^{res} over the networks are defined as I^{rec} and x^{rec}, respectively.

If the DOB functions ideally, the transfer function of the motor with the DOB can be represented as (10)

$$G_n(s) = \frac{x^{res}}{I^{ref}} = \frac{K_{tn}}{M_n s^2}, \tag{10}$$

where K_{tn} and M_n denote the nominal thrust constant and nominal mass of the motor, respectively. For example, the position controller can be configured as (11)

$$\begin{aligned} I^{ref} &= \frac{M_n}{K_{tn}} \ddot{x}^{ref} \\ &= \frac{M_n}{K_{tn}} C_p(s) \left(x^{cmd} - x^{rec} \right), \end{aligned} \tag{11}$$

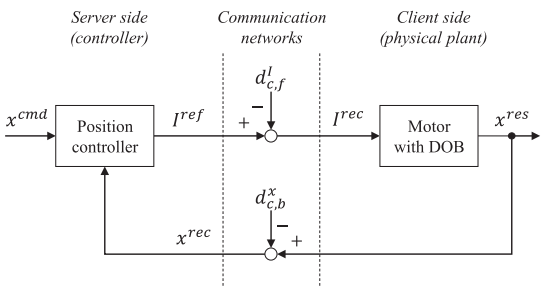

Fig. 10 Remote motor position control system.

where $\ddot{x}^{ref}$ and $C_p(s)$ denote the acceleration reference and the proportional-derivative (PD)-based feedback controller, respectively. The PD-based feedback controller is represented as $C_p(s) = K_p + K_d s$, where K_p and K_d denote the position and velocity feedback gains, respectively.

4.2 System Configuration with CQEO Bank

This study proposes a remote motor position control system using the CQEO-based network control with path diversity. The configuration of the system with two redundant forward and feedback paths is shown in Fig. 11. It is assumed that there is only one controller server in the system, and that there are no server selection algorithms. To improve the reliability of the system, two redundant paths are configured for both forward and feedback networks. The same data are transmitted over the two redundant paths. The communication quality disturbances of forward paths 1 and 2 are defined as $d^I_{c,f1}$ and $d^x_{c,f2}$, respectively. The communication quality disturbances of feedback paths 1 and 2 are defined as $d^I_{c,b1}$ and $d^x_{c,b2}$, respectively.

The path selector determines the combination of forward and feedback paths with the best quality, based on the estimated communication quality disturbance for each path combination (i, j), where $i \in \{1, 2\}$ and $j \in \{1, 2\}$ denote the path numbers of forward and feedback networks, respectively. The CQEO bank comprises multiple CQEOs for all the path combinations $(1, 1)$, $(1, 2)$, $(2, 1)$, and $(2, 2)$, whose outputs are defined as $\hat{d}_{c,1,1}$, $\hat{d}_{c,1,2}$, $\hat{d}_{c,2,1}$, and $\hat{d}_{c,2,2}$, respectively. The current reference selected for the forward network and position response selected for the feedback network are defined as I^{sel} and x^{sel}, respectively. As shown in Fig. 11, the selected current reference I^{sel} takes a value of either I^{rec}_1 or I^{rec}_2, and the selected position response x^{sel} takes a value of either x^{rec}_1 or x^{rec}_2.

4.3 CQEO Bank and Path Selector

As described in Sect. 3, each CQEO estimates the communication quality disturbance for each path combination, $\hat{d}_{c,i,j}$. Since the nominal model of the motor is represented as (10), the disturbance $\hat{d}_{c,i,j}$ can be calculated as (12)

$$\hat{d}_{c,i,j} = G_n(s) d^I_{c,fi} + d^x_{c,bj}, \tag{12}$$

where $d^I_{c,fi}$ and $d^x_{c,bj}$ denote the communication quality disturbances for the i-th forward path and j-th feedback path, respectively.

Although various algorithms of the path selector can be adopted, this paper presents an intuitive algorithm based on the absolute values of $\hat{d}_{c,i,j}$. In a similar way to (9), the selected combination of forward and feedback paths is determined as (13)

$$\arg\min_{i \in \{1,2\}, j \in \{1,2\}} \left| \frac{g_{cqeo}}{s + g_{cqeo}} \hat{d}_{c,i,j} \right|, \tag{13}$$

where the combination (i, j) indicates the path number for

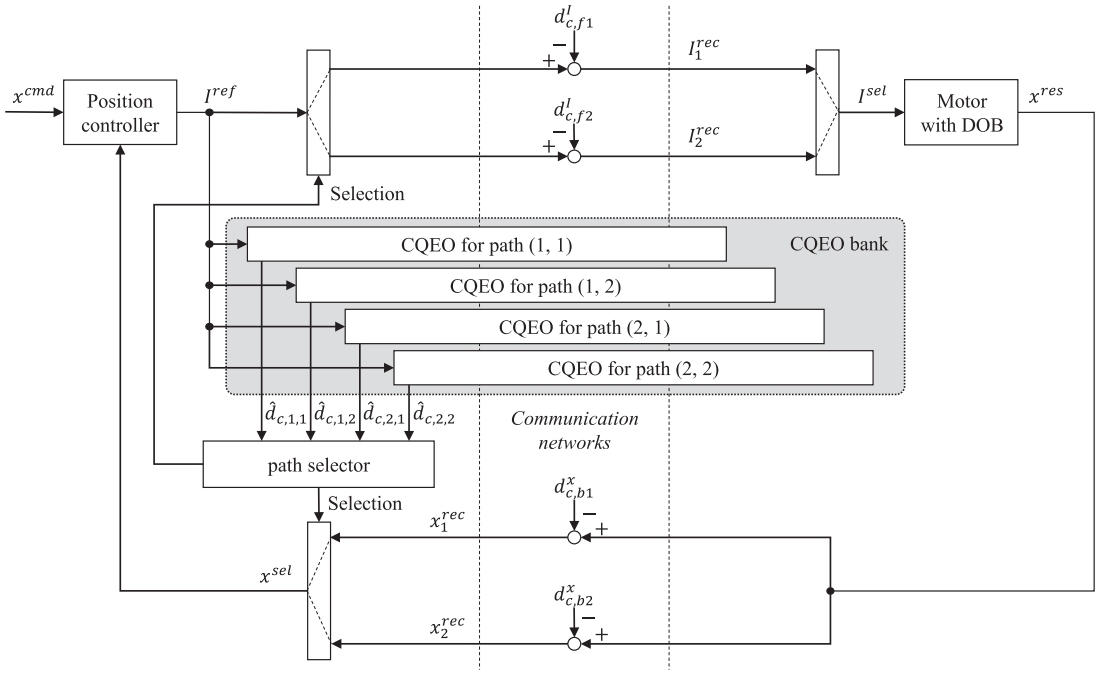

Fig. 11 Remote motor position control with path diversity.

i-th forward path and j-th feedback path. The path selector changes the forward and feedback paths to be used based on the selected combination of the paths.

5. Path Diversity with CQEO for Peer-to-Peer NCSs

This section describes the CQEO-based network control technique using path diversity for the peer-to-peer NCSs by taking a haptic communication system as an example.

5.1 Bilateral Control for Haptic Communication

Bilateral teleoperation system, or haptic communication system, includes master and slave haptic devices and their controllers. The master and slave subsystems are connected over communication networks. In a haptic communication system, a human operator manipulates a master device and can feel the reaction force exerted on a slave device as if she/he is directly touching the remote environment. Haptic communication can be widely utilized in medical, industrial, and consumer applications. Four-channel bilateral control is one of the generalized control architectures to achieve haptic communication [60]. The four-channel bilateral control system over communication networks is shown in Fig. 12.

On the master side, the human operator inputs the external force f_m^{ext} by manipulating the master device. The position and external force of the master device are measured as x_m^{res} and $\hat{f}_m^{ext}$, respectively. On the slave side, the slave device is manipulated in the same trajectory as the master device by the four-channel bilateral controller. If the slave device contacts the remote environment, the external force f_s^{ext} is generated. The position and external force of the slave device are measured as x_s^{res} and $\hat{f}_s^{ext}$, respectively.

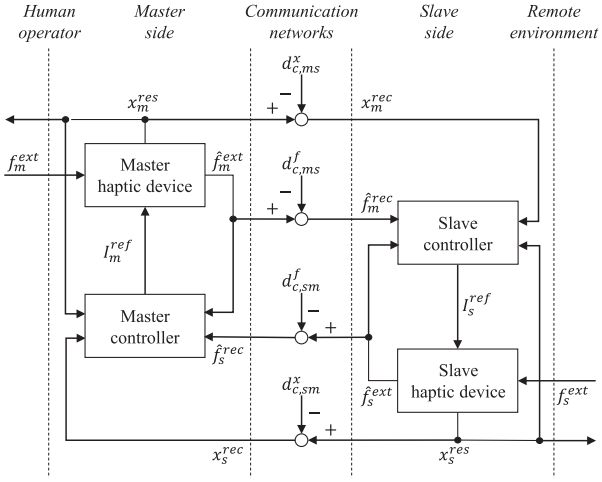

Fig. 12 Four-channel bilateral control system over the networks.

The position and force responses, i.e., x_m^{res}, x_s^{res}, $\hat{f}_m^{ext}$, and $\hat{f}_s^{ext}$, are transmitted over the communication networks to achieve perfect transparency between the master and slave sides. The perfect transparency is defined as (14) and (15)

$$x_m^{res} - x_s^{res} = 0, \tag{14}$$

$$\hat{f}_m^{ext} + \hat{f}_s^{ext} = 0. \tag{15}$$

The communication quality disturbances of the master-to-slave position and force channels and the slave-to-master position and force channels, $d^x_{c,ms}$, $d^f_{c,ms}$, $d^x_{c,sm}$, and $d^f_{c,sm}$, include the effects of time delays, packet losses, and cyber-attacks. It is assumed that the position and force responses are transmitted in the same packet on the master-to-slave and slave-to-master networks. The received values for x_m^{res},

$\hat{f}_m^{ext}$, x_s^{res}, and $\hat{f}_s^{ext}$ over the networks are defined as x_m^{rec}, $\hat{f}_m^{rec}$, x_s^{rec}, and $\hat{f}_s^{rec}$, respectively. In practice, the master and slave velocity responses, $\dot{x}_m^{res}$ and $\dot{x}_s^{res}$, in addition to the position and force responses can be measured. In this case, the velocity response on each side is transmitted over the networks in the same packet as the position and force responses on the corresponding side. The communication quality disturbances and the values received over networks for the velocity response are defined as $d_{c,ms}^{\dot{x}}$ and $\dot{x}_m^{rec}$ on the master-to-slave network, and $d_{c,sm}^{\dot{x}}$ and $\dot{x}_s^{rec}$ on the slave-to-master network, respectively.

In this study, the acceleration-based four-channel bilateral controller [61] is implemented. Current-controlled linear motors with the same nominal mass M_n and nominal thrust constant K_{tn} are utilized for actuating the master and slave haptic devices. The DOB is implemented on each haptic device. If the DOB functions ideally, the transfer function of the master and slave haptic devices with the DOB can be represented as (16)

$$G_n(s) = \frac{x_m^{res}}{I_m^{ref}} = \frac{x_s^{res}}{I_s^{ref}} = \frac{K_{tn}}{M_n s^2}, \tag{16}$$

where I_m^{ref} and I_s^{ref} denote the current references for the master and slave devices, respectively.

The master and slave controllers can be configured as (17) and (18)

$$\begin{aligned} I_m^{ref} &= \frac{M_n}{K_{tn}} \{-C_p(s)(x_m^{res} - x_s^{rec}) \\ &\quad -C_f(\hat{f}_m^{ext} + \hat{f}_s^{rec})\}, \end{aligned} \tag{17}$$

$$\begin{aligned} I_s^{ref} &= \frac{M_n}{K_{tn}} \{-C_p(s)(x_s^{res} - x_m^{rec}) \\ &\quad -C_f(\hat{f}_m^{rec} + \hat{f}_s^{ext})\}, \end{aligned} \tag{18}$$

where $C_p(s) = K_p + K_d s$ and $C_f = K_f$ are the position controller and force controller, respectively. The gains K_p, K_d, and K_f denote the position, velocity, and force feedback gains, respectively.

If there are no communication quality disturbances and the DOB functions ideally, the transparency in the four-channel bilateral control system can be calculated as (19)

$$\begin{bmatrix} \hat{f}_m^{ext} \\ -x_s^{res} \end{bmatrix} = \begin{bmatrix} -\frac{s^2}{C_f} & 1 \\ -1 & 0 \end{bmatrix} \begin{bmatrix} x_m^{res} \\ -\hat{f}_s^{ext} \end{bmatrix}. \tag{19}$$

Therefore, the perfect transparency, i.e., (14) and (15), is achieved if the force feedback gain K_f is sufficiently large.

5.2 System Configuration with Master and Slave CQEOs

In reality, the bilateral control system is affected by the communication quality disturbances. To achieve reliable haptic communication, communication quality estimation and control techniques are required. This study proposes a haptic communication system using the CQEO-based network control with path diversity. The configuration of the system with two redundant master-to-slave and slave-to-master paths is shown in Fig. 13. It is assumed that master and slave devices to be utilized are designated in advance, and this system does not have any peer selection algorithms.

To improve the reliability of the system, two redundant paths are configured for both master-to-slave and slave-to-master networks. The same data are transmitted over the two redundant paths. The vector $\boldsymbol{p}_m^{res} = [x_m^{res}, \dot{x}_m^{res}, \hat{f}_m^{ext}]^T$ is transmitted from the master side to the slave side, and the vector $\boldsymbol{p}_s^{res} = [x_s^{res}, \dot{x}_s^{res}, \hat{f}_s^{ext}]^T$ is transmitted from the slave side to the master side. The communication quality disturbance vectors of master-to-slave paths 1 and 2 are defined as $\boldsymbol{d}_{c,ms1} = [d_{c,ms1}^x, d_{c,ms1}^{\dot{x}}, d_{c,ms1}^f]^T$ and $\boldsymbol{d}_{c,ms2} = [d_{c,ms2}^x, d_{c,ms2}^{\dot{x}}, d_{c,ms2}^f]^T$, respectively. The communication quality disturbance vectors of slave-to-master paths 1 and 2 are defined as $\boldsymbol{d}_{c,sm1} = [d_{c,sm1}^x, d_{c,sm1}^{\dot{x}}, d_{c,sm1}^f]^T$ and $\boldsymbol{d}_{c,sm2} = [d_{c,sm2}^x, d_{c,sm2}^{\dot{x}}, d_{c,sm2}^f]^T$, respectively.

In the bilateral control system, the master-to-slave and slave-to-master networks are evaluated separately because the system has two degrees of freedom, that is, two controllers. The master path selector determines the slave-to-master path with the best quality, based on the communication quality disturbance vector $\hat{\boldsymbol{d}}_{c,m}^x = [\hat{d}_{c,m1}^x, \hat{d}_{c,m2}^x]^T$ estimated by the master CQEO. The slave path selector determines the master-to-slave path with the best quality, based on the communication quality disturbance vector $\hat{\boldsymbol{d}}_{c,s}^x = [\hat{d}_{c,s1}^x, \hat{d}_{c,s2}^x]^T$ estimated by the slave CQEO. The vectors selected for the master-to-slave and slave-to-master networks are defined as $\boldsymbol{p}_m^{sel} = [x_m^{sel}, \dot{x}_m^{sel}, \hat{f}_m^{sel}]^T$ and $\boldsymbol{p}_s^{sel} = [x_s^{sel}, \dot{x}_s^{sel}, \hat{f}_s^{sel}]^T$, respectively. As shown in Fig. 13, the master selected vector $\boldsymbol{p}_m^{sel}$ takes a vector of either $\boldsymbol{p}_{m1}^{rec} = [x_{m1}^{rec}, \dot{x}_{m1}^{rec}, \hat{f}_{m1}^{rec}]^T$ or $\boldsymbol{p}_{m2}^{rec} = [x_{m2}^{rec}, \dot{x}_{m2}^{rec}, \hat{f}_{m2}^{rec}]^T$, and the slave selected vector $\boldsymbol{p}_s^{sel}$ takes a vector of either $\boldsymbol{p}_{s1}^{rec} = [x_{s1}^{rec}, \dot{x}_{s1}^{rec}, \hat{f}_{s1}^{rec}]^T$ or $\boldsymbol{p}_{s2}^{rec} = [x_{s2}^{rec}, \dot{x}_{s2}^{rec}, \hat{f}_{s2}^{rec}]^T$.

5.3 Master and Slave CQEOs and Path Selectors

The master CQEO calculates the estimated disturbances, $\hat{d}_{c,m1}^x$ and $\hat{d}_{c,m2}^x$, as (20) and (21)

$$\hat{d}_{c,m1}^x = x_{s\_model}^{res} - x_{s1}^{rec}, \tag{20}$$

$$\hat{d}_{c,m2}^x = x_{s\_model}^{res} - x_{s2}^{rec}, \tag{21}$$

where $x_{s\_model}^{res}$ denotes the position response of the slave haptic device model on the master side, which includes the position controller $C_p(s)$. The current reference $I_{s\_model}^{ref}$ is calculated as (22)

$$I_{s\_model}^{ref} = \frac{M_n}{K_{tn}} C_p(s)(x_m^{res} - x_{s\_model}^{res}). \tag{22}$$

The position response of the slave haptic device model, $x_{s\_model}^{res}$, can be calculated as (23)

$$x_{s\_model}^{res} = \frac{K_{tn}}{M_n s^2} I_{s\_model}^{ref}. \tag{23}$$

The slave CQEO calculates the estimated disturbances,

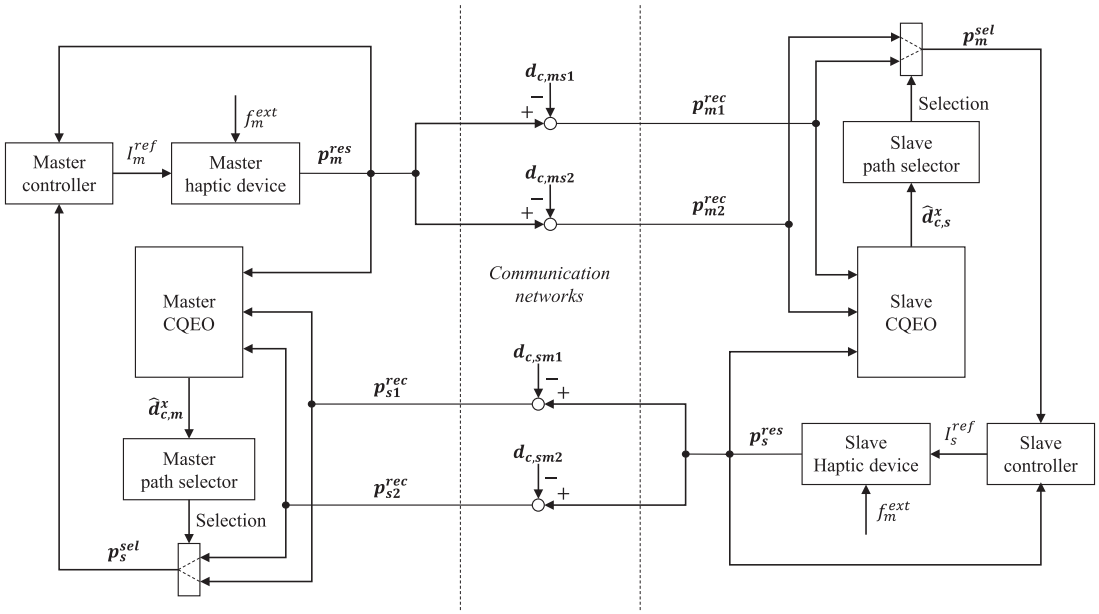

Fig. 13 Haptic communication with path diversity.

$\hat{d}^x_{c,s1}$ and $\hat{d}^x_{c,s2}$, as (24) and (25)

$$\hat{d}^x_{c,s1} = x^{res}_{m\_model} - x^{rec}_{m1}, \tag{24}$$

$$\hat{d}^x_{c,s2} = x^{res}_{m\_model} - x^{rec}_{m2}, \tag{25}$$

where $x^{res}_{m\_model}$ denotes the position response of the master haptic device model on the slave side, which includes the position controller $C_p(s)$. The current reference $I^{ref}_{m\_model}$ is calculated as (26)

$$I^{ref}_{m\_model} = \frac{M_n}{K_{tn}} C_p(s)(x^{res}_s - x^{res}_{m\_model}). \tag{26}$$

The position response of the master haptic device model, $x^{res}_{m\_model}$, can be calculated as (27)

$$x^{res}_{m\_model} = \frac{K_{tn}}{M_n s^2} I^{ref}_{m\_model}. \tag{27}$$

Although various algorithms of the path selectors can be adopted, this study presents an intuitive algorithm based on the absolute values of the communication quality disturbances. In the slave path selector, the selected master-to-slave path is determined as (28)

$$\arg\min_{i\in\{1,2\}} \left| \frac{g_{cqeo}}{s + g_{cqeo}} \hat{d}^x_{c,si} \right|, \tag{28}$$

where i indicates the master-to-slave path number. In the master path selector, the selected slave-to-master path is determined as (29)

$$\arg\min_{j\in\{1,2\}} \left| \frac{g_{cqeo}}{s + g_{cqeo}} \hat{d}^x_{c,mj} \right|, \tag{29}$$

where j indicates the slave-to-master path number.

Table 1 Parameters used in the simulation.

Nominal mass	M_n	0.5	kg
Nominal thrust constant	K_{tn}	32.5	N/A
Position feedback gain	K_p	900	
Velocity feedback gain	K_d	60	
Force feedback gain	K_f	1	
Cut-off frequency of the DOB	g_{dob}	500	rad/s
Cut-off frequency of the RFOB	g_{reac}	500	rad/s
Cut-off frequency of the CQEO	g_{cqeo}	1000	rad/s

6. Simulation

This section shows the simulation results with the haptic communication system to confirm the effectiveness of the communication quality estimation and control using the CQEO.

6.1 Setup

In the simulation, the conventional four-channel control system shown in Fig. 12 and the proposed control system with path diversity shown in Fig. 13 were compared. The parameters used in the simulation are shown in Table 1. The reaction force observers (RFOBs) were implemented to estimate the master and slave external forces without force sensors [62]. The RFOBs calculated the external forces, $\hat{f}^{ext}_m$ and $\hat{f}^{ext}_s$, as (30) and (31)

$$\hat{f}^{ext}_m = \frac{g_{reac}}{s + g_{reac}} f^{ext}_m, \tag{30}$$

$$\hat{f}^{ext}_s = \frac{g_{reac}}{s + g_{reac}} f^{ext}_s, \tag{31}$$

where g_{reac} denotes the cut-off frequency of the first-order LPF. The control period was set to 1 ms. A human operator

Table 2 Network conditions for the system without path diversity.

Cond. No.	Delay	Attack ($0\,\mathrm{s} \le t < 10\,\mathrm{s}$)	Attack ($10\,\mathrm{s} \le t < 20\,\mathrm{s}$)
1	10 ms	×	✓
2	50 ms	×	✓
3	20–80 ms	×	✓

Table 3 Network conditions for the system with path diversity.

Cond. No.	Path No.	Delay	Attack ($0\,\mathrm{s} \le t < 10\,\mathrm{s}$)	Attack ($10\,\mathrm{s} \le t < 20\,\mathrm{s}$)
4	1	50 ms	×	×
	2	10 ms	×	✓
5	1	20–80 ms	×	×
	2	50 ms	×	✓

manipulated the master device so that the slave device would contact the remote environment. The mechanical impedance of the human operator Z_h, which indicates the relationship between the master external force f_m^{ext} and master velocity response $\dot{x}_m^{res}$, was set to $50/s + 10\,\mathrm{N{\cdot}s/m}$. The position of environment was set to 0.01 m on the slave side. The mechanical impedance of the remote environment Z_e, which indicates the relationship between the slave external force f_s^{ext} and slave velocity response $\dot{x}_s^{res}$ in contact motion, was set to $1000/s + 10\,\mathrm{N{\cdot}s/m}$.

The target of haptic communication is that master and slave position responses take the same value and master and slave force responses follow the law of action and reaction, as shown in (14) and (15). The time delays and data tampering attacks on the master-to-salve and slave-to-master networks were given as the five network conditions shown in Tables 2 and 3, where t denotes the elapsed time. The random jitters followed the uniform distribution in the designated range. The data tampering attacks were injected as an additive disturbance d_a on each position, velocity, and force channel over the master-to-slave and slave-to-master networks. Disturbance d_a was set to a random number ranged from 0 to 0.001 at intervals of 10^{-5} followed uniform distribution. The disturbance is small relative to the range of motion. However, in haptic communication systems, a small displacement can generate a large reaction force when the slave haptic device has contact with a hard object. This is a critical problem if the system is applied to the services involving human lives such as telesurgery. This kind of attacks can be achieved as a man-in-the-middle attack. The simulations assumed that there were no packet losses on the networks. The same network condition was applied to both master-to-slave and slave-to-master networks in the same simulation.

6.2 Results

The simulation results without path diversity for conditions 1, 2, and 3 are shown in Figs. 14–16, respectively. The master and slave position responses under conditions 1, 2, and 3 are shown in Figs. 14(a), 15(a), and 16(a), respectively. The master and slave force responses under conditions 1, 2, and 3 are shown in Figs. 14(b), 15(b), and 16(b), respectively. In these conditions, only one path was configured for each of master-to-slave and slave-to-master network.

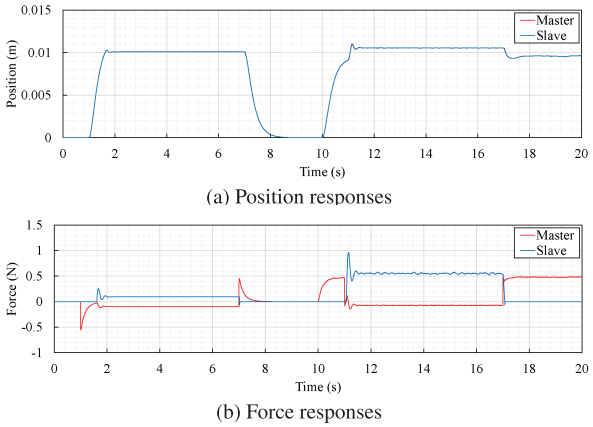

(a) Position responses

(b) Force responses

Fig. 14 Simulation results without path diversity (Condition 1).

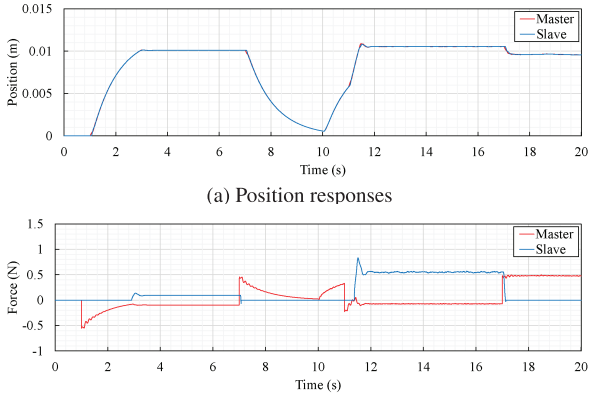

(a) Position responses

(b) Force responses

Fig. 15 Simulation results without path diversity (Condition 2).

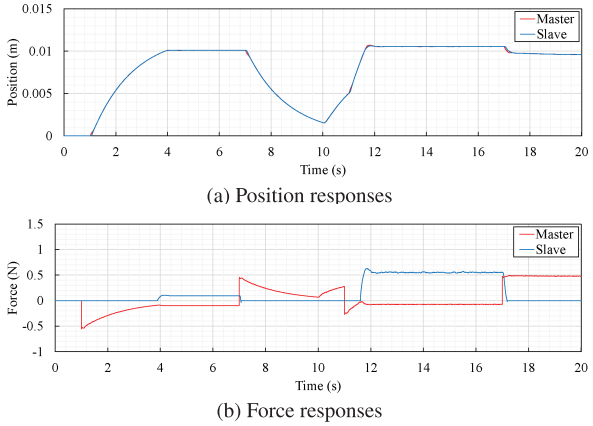

(a) Position responses

(b) Force responses

Fig. 16 Simulation results without path diversity (Condition 3).

It is clear from Fig. 14 that the position and force responses achieved high-transparency haptic communication, that is, (14) and (15), for the first 10 s while generating the impulsive operational force of approximately −0.5 N at 1 s

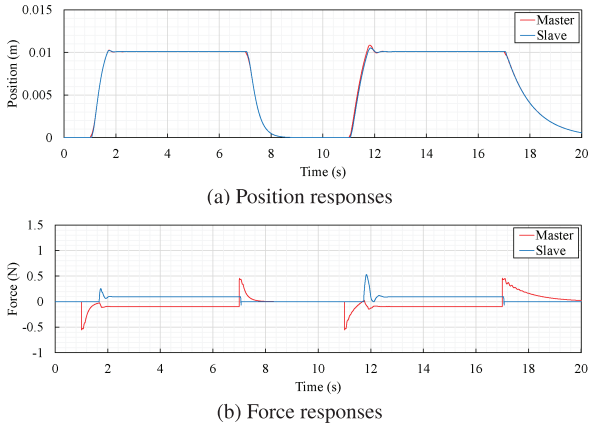

(a) Position responses

(b) Force responses

Fig. 17 Simulation results with path diversity (Condition 4).

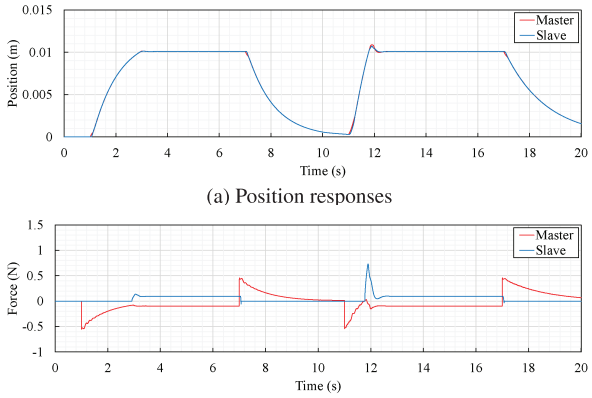

(a) Position responses

(b) Force responses

Fig. 18 Simulation results with path diversity (Condition 5).

on the master side. The operational force was generated because the master device did not start moving immediately due to the time delays even if the human operator applied force to the master device. As shown in Fig. 15, the results had slower response times than those of condition 1 because the delay was set to a larger value than that of condition 1. As shown in Fig. 16, the results had slower response times than those of condition 2 because the delay had jitter and the maximum delay was set to 80 ms. In conditions 1–3, after 10 s, the master and slave force responses did not satisfy (15) because of data tampering attacks. In addition, the force responses fluctuated after 10 s, which means that the operator felt the persistent oscillations. Therefore, the systems without path diversity were directly affected by the time delays and data tampering attacks shown in Table 2, because they do not contain any redundant paths.

The simulation results with path diversity for conditions 4 and 5 are shown in Figs. 17 and 18, respectively. The master and slave position responses under conditions 4 and 5 are shown in Figs. 17(a) and 18(a), respectively. The master and slave force responses under conditions 4 and 5 are shown in Figs. 17(b) and 18(b), respectively. In these conditions, two paths were configured for each of master-to-slave and slave-to-master network. In addition, the CQEO and path selector were implemented on each of the master and slave sides.

As confirmed by Figs. 17 and 18, regardless of the presence or absence of the data tampering attacks, the position and force responses achieved high-transparency haptic communication, that is, (14) and (15), while generating the impulsive operational force of approximately −0.5 N at 1 s and 11 s on the master side. As shown in Fig. 17, the results had almost the same response time as those of condition 1 because the path selectors could mainly choose path 2 with a 10-ms delay for the first 10 s. As shown in Fig. 18, the results had almost the same response time as those of condition 2 because the path selectors could mainly choose path 2 with a 50-ms delay for the first 10 s. Therefore, the proposed system with path diversity provided higher transparency than the conventional system without path diversity, because it could select an appropriate path and avoid the critical effect of the communication quality disturbance including time delays, jitters, and data tampering attacks based on the estimation of the integrated communication quality at the application level.

7. Conclusion and Future Directions

We described the concept, methodology, and applications of the integrated communication quality estimation and control for the DT-assisted CPSs from both communications and control perspectives. The DT-assisted CPSs were modelled as client-server and peer-to-peer NCSs. Furthermore, we presented the application-level communication quality control using the CDOB and the network-level communication quality control using the CQEO. We also discussed the specific configurations of the CQEO for the client-server and peer-to-peer NCSs by taking the remote motor control and haptic communication systems as examples, respectively. The simulation results showed the effectiveness of the CQEO-based network control technique for the haptic communication system.

In the beyond-5G/6G era, the current MEC-based architecture for delay-sensitive applications will migrate to a co-created multi-access anywhere computing (CMAC) architecture. Distributed computing and network resources will be virtualized and selectively utilized by the applications to achieve the best communication quality. The CMAC architecture provides the communication quality co-created by not only networks and applications but also users, because the CPSs will evolve into cyber-physical-social systems (CPSSs) including human activities [63]. The quality of experiences (QoE) is an index to measure user experiences for network applications [64]. A real-time QoE feedback scheme for network and application control accelerates the research and development of the CMAC-based CPSSs. Therefore, the estimation and control scheme of the integrated communication quality at the human perception level is required to realize future DT-assisted CPSSs.

Acknowledgments

This work was supported in part by JSPS KAKENHI Grant Number 18K11275 and Keio Gijuku Academic Development Funds. The author would like to thank laboratory members for their fruitful discussions.

References

[1] K.-D. Kim and P.R. Kumar, "Cyber-physical systems: A perspective at the centennial," Proc. IEEE, vol.100, pp.1287–1308, May 2012. DOI: 10.1109/JPROC.2012.2189792
[2] D. Baumann, F. Mager, U. Wetzker, L. Thiele, M. Zimmerling, and S. Trimpe, "Wireless control for smart manufacturing: Recent approaches and open challenges," Proc. IEEE, vol.109, no.4, pp.441–467, April 2021. DOI: 10.1109/JPROC.2020.3032633
[3] J. Baillieul and P. J. Antsaklis, "Control and communication challenges in networked real-time systems," Proc. IEEE, vol.95, no.1, pp.9–28, Jan. 2007. DOI: 10.1109/JPROC.2006.887290
[4] R. A. Gupta and M.-Y. Chow, "Networked control system: Overview and research trends," IEEE Trans. Ind. Electron., vol.57, no.7, pp.2527–2535, July 2010. DOI: 10.1109/TIE.2009.2035462
[5] X. Zhang, Q. Han, X. Ge, D. Ding, L. Ding, D. Yue, and C. Peng, "Networked control systems: A survey of trends and techniques," IEEE/CAA J. Autom. Sinica, pp.1–17, July 2019. DOI: 10.1109/JAS.2019.1911651
[6] L. Zhang, H. Gao, and O. Kaynak, "Network-induced constraints in networked control systems — A survey," IEEE Trans. Ind. Informat., vol.9, no.1, pp.403–416, Feb.2013. DOI: 10.1109/TII.2012.2219540
[7] P. Park, S.C. Ergen, C. Fischione, C. Lu, and K. H. Johansson, "Wireless network design for control systems: A survey," IEEE Commun. Surveys Tuts., vol.20, no.2, pp.978–1013, Secondquarter 2018. DOI: 10.1109/COMST.2017.2780114
[8] H. Ishii and K. Tsumura, "Data rate limitations in feedback control over networks," IEICE Trans. Fundamentals., vol.E95-A, no.4, pp.680–690, April 2012. DOI: 10.1587/transfun.E95.A.680
[9] M. Nagahara, T. Matsuda, and K. Hayashi, "Compressive sampling for remote control systems," IEICE Trans. Fundamentals, vol.E95-A, no.4, pp.713–722, April 2012. DOI: 10.1587/transfun.E95.A.713
[10] T. Iwai, D. Kominami, M. Murata, R. Kubo, and K. Satoda, "Mobile network architectures and context-aware network control technology in the IoT era," IEICE Trans. Commun., vol.E101-B, no.10, pp.2083–2093, Oct. 2018. DOI: 10.1587/transcom.2017NEI0001
[11] K. Kobayashi, H. Okada, and M. Katayama, "A cross-layer optimized receiver design for wireless feedback control systems," IEEE Trans. Commun., vol.66, no.1, pp.320–329, Jan. 2018. DOI: 10.1109/TCOMM.2017.2751472
[12] K. Nakashima, T. Matsuda, M. Nagahara, and T. Takine, "Multi-hop TDMA-based wireless networked control systems robust against bursty packet losses: A two-path approach," IEICE Trans. Commun., vol.E103-B, no.3, pp. 200–210, March 2020. DOI: 10.1587/transcom.2019EBP3110
[13] ITU-T Technology Watch Report, "The Tactile Internet," Aug. 2014.
[14] A. Aijaz and M. Sooriyabandara, "The Tactile Internet for industries: A review," Proc. IEEE, vol.107, no.2, pp.414–435, Feb. 2019. DOI: 10.1109/JPROC.2018.2878265
[15] E. Wong, M.P.I. Dias, and L. Ruan, "Predictive resource allocation for Tactile Internet capable passive optical LANs," J. Lightw. Technol., vol.35, no.13, pp.2629–2641, July 2017. DOI: 10.1109/JLT.2017.2654365
[16] R. Imai and R. Kubo, "Cloud-based remote motion control over FTTH networks for home robotics," Proc. 3rd IEEE Global Conf. Consumer Electronics (GCCE), pp.565–566, Oct.2014. DOI: 10.1109/GCCE.2014.7031107
[17] R. Kubo, T. Michigami, K. Yamada, and M. Yoshino, "Demonstration of wide-area networked motion control over long-reach 10G-EPON based on optical access edge computing," Proc. 24th OptoElectronics and Communications Conf./Int. Conf. Photonics in Switching and Computing 2019 (OECC/PSC), TuA3-5, July 2019. DOI: 10.23919/PS.2019.8817734
[18] M. Maier and A. Ebrahimzadeh, "Towards immersive Tactile Internet experiences: Low-latency FiWi enhanced mobile networks with edge intelligence," J. Opt. Commun. Netw., vol.11, no.4, pp.B10–B25, April 2019. DOI: 10.1364/JOCN.11.000B10
[19] S.K. Sharma, I. Woungang, A. Anpalagan, and S. Chatzinotas, "Toward Tactile Internet in beyond 5G era: Recent advances, current issues, and future directions," IEEE Access, vol.8, pp.56948–56991, 2020. DOI: 10.1109/ACCESS.2020.2980369
[20] K.-J. Park, J. Kim, H. Lim, and Y. Eun, "Robust path diversity for network quality of service in cyber-physical systems," IEEE Trans. Ind. Informat., vol.10, no.4, pp.2204–2215, Nov. 2014. DOI: 10.1109/TII.2014.2351753
[21] K. Terai, D. Anzai, K. Lee, K. yanagihara, and S. Hara, "A distant multipath routing method for reliable wireless multi-hop data transmission," IEICE Trans. Fundamentals., vol.E95-A, no.4, pp.723–734, April 2012. DOI: 10.1587/transfun.E95.A.723
[22] C. Tan, W. S. Wong, H. Zhang, and Z. Zhang, "Integrated stabilisation policy over multipath routing-enabled network," IET Control Theory Appl., vol.14, no.19, pp.3312–3319, Dec. 2020. DOI: 10.1049/iet-cta.2020.0312
[23] R. Jiang and X. Zhang, "Application of wireless network control to course-keeping for ships," IEEE Access, vol.8, pp.31674–31683, 2020. DOI: 10.1109/ACCESS.2020.2973464
[24] C.-H. Chen, C.-L. Lin, and T.-S. Hwang, "Stability of networked control systems with time-varying delays," IEEE Commun. Lett., vol.11, no.3, pp.270–272, March 2007. DOI: 10.1109/LCOMM.2007.060716
[25] N. Vatanski, J.-P. Georges, C. Aubrun, E. Rondeau, and S.-L. Jämsä-Jounela, "Networked control with delay measurement and estimation," Control Eng. Pract., vol.17, no.2, pp.231–244, Feb. 2009. DOI: 10.1016/j.conengprac.2008.07.004
[26] C.-L. Lai and P.-L. Hsu, "Design the remote control system with the time-delay estimator and the adaptive Smith predictor," IEEE Trans. Ind. Informat., vol.6, no.1, pp.73–80, Feb. 2010. DOI: 10.1109/TII.2009.2037917
[27] A. Fuller, Z. Fan, C. Day, and C. Barlow, "Digital twin: Enabling technologies, challenges and open research," IEEE Access, vol.8, pp.108952–108971, 2020. DOI: 10.1109/ACCESS.2020.2998358
[28] A. Rasheed, O. San, and T. Kvamsdal, "Digital twin: Values, challenges and enablers from a modeling perspective," IEEE Access, vol.8, pp.21980–22012, 2020. DOI: 10.1109/ACCESS.2020.2970143
[29] M. Groshev, C. Guimarães, J. Martín-Pérez, and A. Oliva, "Toward intelligent cyber-physical systems: Digital twin meets artificial intelligence," IEEE Commun. Mag., vol.59, no.8, pp.14–20, Aug. 2021. DOI: 10.1109/MCOM.001.2001237
[30] S.R. Newrzella, D.W. Franklin, and S. Haider, "5-dimension cross-industry digital twin applications model and analysis of digital twin classification terms and models," IEEE Access, vol.9, pp.131306–131321, 2021. DOI: 10.1109/ACCESS.2021.3115055
[31] R. Zhao, D. Yan, Q. Liu, J. Leng, J. Wan, X. Chen, and X. Zhang, "Digital twin-driven cyber-physical system for autonomously controlling of micro punching system," IEEE Access, vol.7, pp.9459–9469, 2019. DOI: 10.1109/ACCESS.2019.2891060
[32] W. Yang, Y. Zheng, and S. Li, "Application status and prospect of digital twin for on-orbit spacecraft," IEEE Access, vol.9, pp.106489–106500, 2021. DOI: 10.1109/ACCESS.2021.3100683
[33] A. Saad, S. Faddel, T. Youssef, and O.A. Mohammed, "On the implementation of IoT-based digital twin for networked microgrids resiliency against cyber attacks," IEEE Trans. Smart Grid, vol.11, no.6, pp.5138–5150, Nov. 2020. DOI: 10.1109/TSG.2020.3000958

[34] K. Natori and K. Ohnishi, "A design method of communication disturbance observer for time-delay compensation, taking the dynamic property of network disturbance into account," IEEE Trans. Ind. Electron., vol.55, no.5, pp.2152–2168, May 2008. DOI: 10.1109/TIE.2008.918635

[35] K. Natori, R. Oboe, and K. Ohnishi, "Stability analysis and practical design procedure of time delayed control systems with communication disturbance observer," IEEE Trans. Ind. Informat., vol.4, no.3, pp.185–197, Aug. 2008. DOI: 10.1109/TII.2008.2002705

[36] W. Zhang, M. Tomizuka, P. Wu, Y. Wei, Q. Leng, S. Han, and A.K. Mok, "A double disturbance observer design for compensation of unknown time delay in a wireless motion control system," IEEE Trans. Control Syst. Technol., vol.26, no.2, pp.675–683, March 2018. DOI: 10.1109/TCST.2017.2665967

[37] C. Süülker and M.T. Emirler, "Comparison of different time delay compensation methods for networked DC motor speed control," Proc. 6th International Conference on Electrical and Electronics Engineering (ICEEE), pp.225–229, April 2019. DOI: 10.1109/ICEEE2019.2019.00050

[38] A. Codrean, O. Stefan, and T.-L. Dragomir, "Design, analysis and validation of an observer-based delay compensation structure for a network control system," Proc. 20th Mediterranean Conf. Control & Automation (MED), pp.928–934, July 2012. DOI: 10.1109/MED.2012.6265757

[39] T. Ogura, K. Kobayashi, H. Okada, and M. Katayama, "H-infinity control design considering packet loss as a disturbance for networked control systems," IEICE Trans. Fundamentals, vol.E100-A, no.2, pp.353–360, Feb. 2017. DOI: 10.1587/transfun.E100.A.353

[40] R. Kubo and K. Natori, "Dependable networked motion control using communication disturbance observer," Proc. 27th Int. Technical Conf. Circuits/Systems, Computers and Communications (ITC-CSCC), D-T1-05, pp.1–4, July 2012.

[41] R. Imai and R. Kubo, "Experimental validation of communication disturbance observer for networked control systems with information losses," IEICE Commun. Express, vol.5, no.4, pp.102–107, April 2016. DOI: 10.1587/comex.2016XBL0015

[42] S. Hyodo and K. Ohnishi, "A method for allocation of system model in communication disturbance observer considering unstable network," IEEJ Trans. Ind. Appl., vol.135, no.3, pp.192–198, March 2015 (in Japanese) DOI: 10.1541/ieejias.135.192

[43] T. Suhara, H. Norizuki, and Y. Uchimura, "Control system design considering packet loss and variable time delay in a network-based system," IEEJ Trans. Ind. Appl., vol.137, no.2, pp. 87–94, Feb. 2017 (in Japanese). DOI: 10.1541/ieejias.137.87

[44] T. Yamanaka, K. Yamada, R. Hotchi, and R. Kubo, "Simultaneous time-delay and data-loss compensation for networked control systems with energy-efficient network interfaces," IEEE Access, vol.8, pp.110082–110092, 2020. DOI: 10.1109/ACCESS.2020.3001293

[45] J.S. Lee, T.-C. Chien, D.-H. Jian, Y.-H. Sun, "A comparative study of communication disturbance observers for time-delay systems," Proc. 9th IEEE Conference on Industrial Electronics and Applications (ICIEA), pp.616–620, June 2014. DOI: 10.1109/ICIEA.2014.6931237

[46] K. Murata, "Network quality estimation for robot control using post-disaster ad hoc communication," Graduation Thesis, Keio University, March 2021.

[47] D. Ding, Q.-L. Han, Y. Xiang, X. Ge, and X.-M. Zhang, "A survey on security control and attack detection for industrial cyber-physical systems," Neurocomputing, vol.275, pp.1674–1683, Jan. 2018. DOI: 10.1016/j.neucom.2017.10.009

[48] M.S. Chong, H. Sandberg, and A.M.H. Teixeira, "A tutorial introduction to security and privacy for cyber-physical systems," Proc. 18th European Control Conference (ECC), pp.968–978, June 2019. DOI: 10.23919/ECC.2019.8795652

[49] J. Hoshino, H. Kojima, T. Funakoshi, R. Imai, and R. Kubo, "Secure networked motion control using tampering detection observer," Proc. 31st Int. Technical Conf. Circuits/Systems, Computers and Communications (ITC-CSCC), pp.613–616, July 2016. DOI: 10.34385/proc.61.5175

[50] J. Hoshino, T. Funakoshi, K. Yamada, and R. Kubo, "Networked motion control with tamper detection observer and Smith predictor," Proc. Int. Symp. Nonlinear Theory and its Applications (NOLTA), pp.62–65, Dec. 2017. DOI: 10.34385/proc.29.A1L-D-2

[51] P. Huang and Y. Ishibashi, "QoS control and QoE assessment in multi-sensory communications with haptics," IEICE Trans. Commun., vol.E96-B, no.2, pp.392–403, Feb. 2013. DOI: 10.1587/transcom.E96.B.392

[52] K. Natori, T. Tsuji, K. Ohnishi, A. Hace, and K. Jezernik, "Time-delay compensation by communication disturbance observer for bilateral teleoperation under time-varying delay," IEEE Trans. Ind. Electron., vol.57, no.3, pp.1050–1062, March 2010. DOI: 10.1109/TIE.2009.2028337

[53] R. Kubo, "Detection and mitigation of false data injection attacks for secure interactive networked control systems," Proc. IEEE Int. Conf. Intelligence and Safety for Robotics (ISR), pp.7–12, Aug. 2018. DOI: 10.1109/IISR.2018.8535978

[54] R. Kubo, "Effects of time delays on observer-based cyberattack detection in interactive networked control systems," Proc. IEEE Int. Conf. Consumer Electronics-Taiwan (ICCE-TW), pp.1–2, May 2019. DOI: 10.1109/ICCE-TW46550.2019.8991857

[55] N. Suzuki and S. Katsura, "Data transmission with multiple-routes for wireless haptic communication system," Proc. 12th IEEE Int. Workshop on Advanced Motion Control (AMC), pp.1–6, March 2012. DOI: 10.1109/AMC.2012.6197095

[56] N. Higo, T. Tsubaki, Y. Sueda, T. Kuwahara, and A. Koike, "Multi-path and compressed data transmission for haptics media communication in robotic system," Proc. 2018 IEEE Int. Symp. Local and Metropolitan Area Networks (LANMAN), pp.127–128, June 2018. DOI: 10.1109/LANMAN.2018.8475053

[57] R. Kubo, K. Natori, and K. Ohnishi, "Network-centric bilateral control architecture for ubiquitous haptic communications," Papers of the IEEJ Technical Meeting on Industrial Instrumentation and Control, IIC-09-57, pp.71–76, March 2009.

[58] K. Ohnishi, M. Shibata, and T. Murakami, "Motion control for advanced mechatronics," IEEE/ASME Trans. Mechatron., vol.1, no.1, pp.56–67, March 1996. DOI: 10.1109/3516.491410

[59] W.-H. Chen, J. Yang, L. Guo, and S. Li, "Disturbance-observer-based control and related methods—An overview," IEEE Trans. Ind. Electron., vol.63, no.2, pp.1083–1095, Feb. 2016. DOI: 10.1109/TIE.2015.2478397

[60] D.A. Lawrence, "Stability and transparency in bilateral teleoperation," IEEE Trans. Robot. Autom., vol.9, no.5, pp.624–637, Oct. 1993. DOI: 10.1109/70.258054

[61] K. Ohnishi, S. Katsura, and T. Shimono, "Motion control for real-world haptics," IEEE Ind. Electron. Mag., vol.4, no.2, pp.16–19, June 2010. DOI: 10.1109/MIE.2010.936761

[62] T. Murakami, F. Yu and K. Ohnishi, "Torque sensorless control in multidegree-of-freedom manipulator," IEEE Trans. Ind. Electron., vol.40, no.2, pp.259–265, April 1993. DOI: 10.1109/41.222648

[63] Y. Zhou, F.R. Yu, J. Chen, and Y. Kuo, "Cyber-physical-social systems: A state-of-the-art survey, challenges and opportunities," IEEE Commun. Surv. Tut., vol.22, no.1, pp.389–425, Firstquarter 2020. DOI: 10.1109/COMST.2019.2959013

[64] T. Yamazaki, "Quality of experience (QoE) studies: Present state and future prospect," IEICE Trans. Commun., vol.E104-B, no.7, pp.716–724, July 2021. DOI: 10.1587/transcom.2020CQI0003

Ryogo Kubo received his B.E. degree in system design engineering and his M.E. and Ph.D. degrees in integrated design engineering from Keio University, Japan, in 2005, 2007, and 2009, respectively. In 2007, he joined the NTT Access Network Service Systems Laboratories, NTT Corporation, Japan. Since 2010, he has been with Keio University, Japan, where he is currently an Associate Professor at the Department of Electronics and Electrical Engineering. From 2019 to 2020, he also held the position of Honorary Research Fellow at the Department of Electronic and Electrical Engineering, University College London (UCL), UK. His research interests include system control, communication systems, networking, and cyber-physical systems. He is a Member of the Institute of Electrical and Electronics Engineers (IEEE), Optica, the Institute of Electrical Engineers of Japan (IEEJ), the Institute of Electronics, Information and Communication Engineers (IEICE), and the Society of Instrument and Control Engineers (SICE). He received the Best Paper Award from the IEICE Communications Society in 2011, the IEEE International Conference on Communications (ICC '12) Best Paper Award in 2012, the Leonard G. Abraham Prize from the IEEE Communications Society in 2013, the 2018 IEEE International Conference on Intelligence and Safety for Robotics (ISR '18) Best Paper Award in 2018, and the Invited Paper Award from the IEICE Electronics Society in 2021.